ACS OMEGA

http://pubs.acs.org/journal/acsodf

Article

Ionically Tagged Magnetic Nanoparticles with Urea Linkers: Application for Preparation of 2-Aryl-quinoline-4-carboxylic Acids via an Anomeric-Based Oxidation Mechanism

Parvin Ghasemi, Meysam Yarie,* Mohammad Ali Zolfigol,* Avat Arman Taherpour,* and Morteza Torabi

Cite This: *ACS Omega* 2020, 5, 3207−3217

Read Online

ACCESS | Metrics & More | Article Recommendations | Supporting Information

ABSTRACT: In this exploration, we reported the design and synthesis of a novel ionically tagged magnetic nanoparticles bearing urea linkers, namely, Fe_3O_4@SiO_2@$(CH_2)_3$−urea−thiazole sulfonic acid chloride. The structure of the mentioned compound was fully characterized by using several techniques including Fourier transform infrared spectroscopy, energy-dispersive X-ray analysis, elemental mapping analysis, thermogravimetric analysis/differential thermal analysis, scanning electron microscopy, transmission electron microscopy, and vibrating sample magnetometer. In the presence of the novel reusable catalyst, applied starting materials including aryl aldehydes, pyruvic acid, and 1-naphthylamine condensed to afford the desired 2-aryl-quinoline-4-carboxylic acid derivatives via an anomeric-based oxidation pathway under solvent-free conditions.

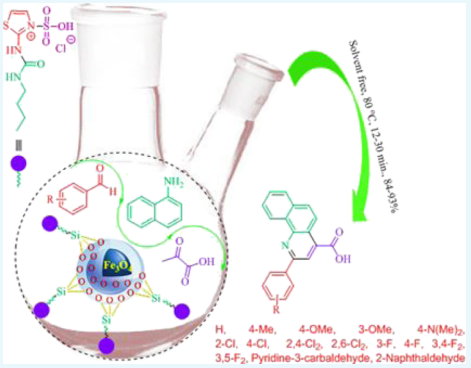

1. INTRODUCTION

Heterocyclic compounds bearing quinoline (benzo[*b*]-pyridine) core are time honored roomy class of organic structures which represent a variety of pharmacological potentialities. Quinoline is an influential pharmacophore in the medicinal chemistry and embraces diverse activities such as antimalarial, antibacterial, antifungal, antitubercular, antitumor, anticancer, anti-HIV, antiprotozoal, anti-inflammatory, anti-proliferative, antioxidant, DNA binding, and antihypertensive. Also, these structures are found to be active in agrochemical chemistry, dye molecules, and coordination chemistry.[1−7] Scheme 1, portrayed some natural products and synthetic drugs with a quinoline core.

Among quinoline structural kernel, 2-aryl-quinoline-4-carboxylic has a quite elegant position. They have been applied as immunosuppressive agents, neurokinin receptor antagonists, mosquito repellant, antiviral, antimicrobial agents, and industrial antioxidants.[8,9] Also, these versatile molecules, applied as key precursors for the construction of other quinolone-based biological active structures.[10] Because of these versatilities, some protocols reported for the synthesis of 2-aryl-quinoline-4-carboxylic acids.[10−19] For example, the Doebner synthesis of quinoline-4-carboxylic derivatives had been adapted to the solid phase.[11b] Although, these methods resolved some issues in the way of 2-aryl-quinoline-4-carboxylic acids, but they connected with some difficulties including long reaction times, using unsafe organic solvents, low yields, and rough reaction conditions. Therefore, presenting new, mild, and convenient synthetic protocols for their preparation are quite valuable.

In the green chemistry domain, catalysis is a key element. Nowadays, because of the environmental concerns associated with chemical synthesis, preparation, and application of eco-friendly and compassionate catalytic systems are the most urgent need of chemists. On the other hand, it is clear that "catalyst activity" and "catalyst separation" are two critical factors in the knowledge of catalysis, and the professional chemists are seeking catalytic systems which embrace these two factors together. Compared with traditional homogeneous and heterogeneous catalytic systems, with nanocatalysis in hand, chemists are working on approaching these factors. These semiheterogeneous catalysts present a large surface-to-volume ratio which is a great solution to boost catalysts activity. To overcome the difficulties of catalysts separation, using magnetic nanoparticles is the most reasonable solution. Therefore, with a combination of nanoscience and catalysis, chemists can design and apply catalytic species which inherit both "catalyst activity" and "catalyst separation" concurrently.[20−28]

Received: October 4, 2019
Accepted: January 29, 2020
Published: February 11, 2020

https://dx.doi.org/10.1021/acsomega.9b03277
ACS Omega 2020, 5, 3207−3217

Scheme 1. Some Natural Products and Synthetic Drug-Bearing Quinoline Core

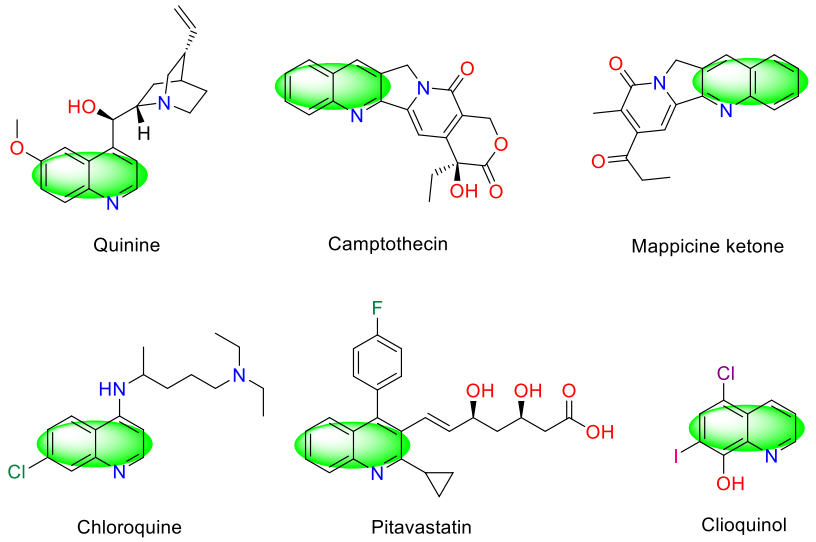

In order to achieve "ideal synthesis", chemists applied a multicomponent reaction (MCR) strategy as a fundamental synthetic tool. MCR behavior represents varied fascinating features which guarantee its position in the green chemistry area. These features are including convergent one-pot reaction processes, less aggressive reaction conditions to the environment, quick access to a library of complex molecules and time, atom, and step economy.[29−37]

Anomeric effect as an important stereoelectronic interaction has an influential role to justify some unusual phenomena in the chemistry knowledge. For example, in the case of 2-fluoro-4,4,5,5-tetramethyl-1,3-dioxole, dynamic nuclear magnetic resonance discloses the hidden ionicity. In this molecule, because of the cooperative anomeric effect of two oxygen atoms; the fluorine atom which exists at the anomeric position quickly shifts from one face of the ring to the opposite face (Scheme 2).[38]

Scheme 2. Anomeric Effect Leads to Hidden Iconicity in 2-Fluoro-4,4,5,5-tetramethyl-1,3-dioxole

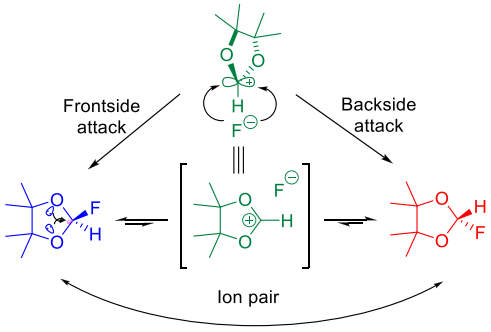

Another fascinating feature of anomeric effect is the capability of bond weakening.[39] Also, cooperativity of anomeric effects (double anomeric effect) can explain some intriguing experimental observations. This case occurred when more than one donor and an acceptor are germinal and exist in a single molecule such as cyclic hemi-orthoesters. In this case, each conformers lead to a different product (Scheme 3).[40]

One of the important subsets of the anomeric effect is the vinylogous anomeric effect.[41−48] In the vinylogous anomeric

Scheme 3. Cooperative Anomeric Effect in the Hydrolysis of Cyclic Hemi-Orthoesters

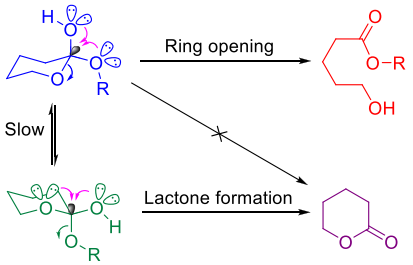

effect, donors interact with acceptors through double bonds.[40] This phenomenon is responsible for the pseudoaxial orientation of the acyloxy group at C-3 in a glycal.[49] Scheme 4, shows the structural outcome of the cooperative vinylogous

Scheme 4. Cooperative Vinylogous Anomeric Effect Leads to Elongation to Exocyclic C−N Bond

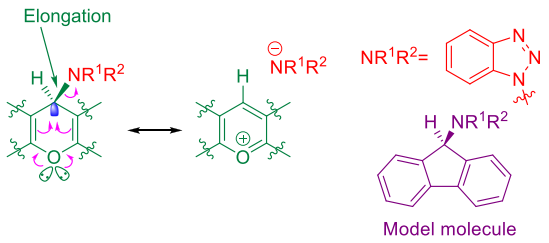

anomeric effect which leads to elongation to an exocyclic C−N bond compared with the C−N bond of the model molecule without the oxygen atom.[50]

In continuation of our efforts to develop catalysts bearing a urea moiety,[51−54] this exploration describes the facile synthesis of 2-aryl-quinoline-4-carboxylic acid derivatives in the presence of a catalytic amount of novel Fe_3O_4@SiO_2@$(CH_2)_3$−urea−thiazole sulfonic acid chloride relying on the expansion of our recently established concept, namely, anomeric-based oxidation (Scheme 5 and 6).[55−62]

https://dx.doi.org/10.1021/acsomega.9b03277
ACS Omega 2020, 5, 3207−3217

Scheme 5. Preparation Route to Fe_3O_4@SiO_2@$(CH_2)_3$−Urea−Thiazole Sulfonic Acid Chloride

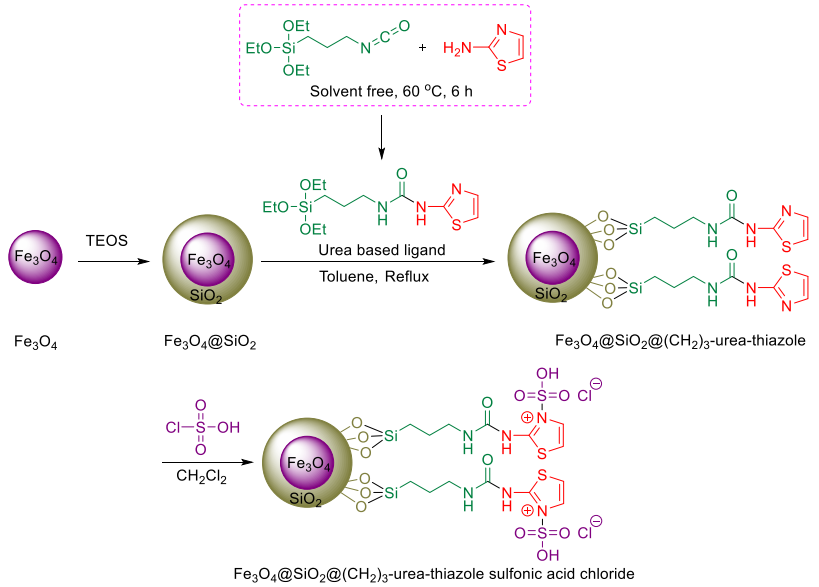

Scheme 6. Catalytic Synthesis of 2-Aryl-quinoline-4-carboxylic Acids

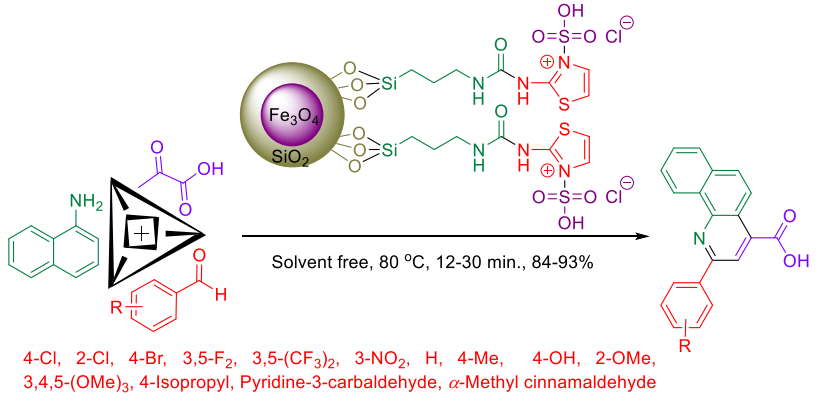

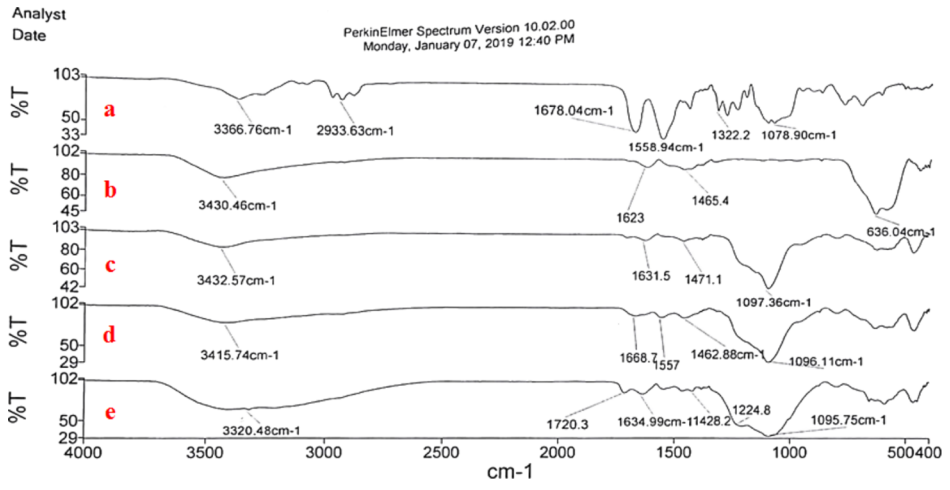

Figure 1. Comparative study of FT-IR spectra of urea-based ligand (a), Fe_3O_4 (b), Fe_3O_4@SiO_2 (c), Fe_3O_4@SiO_2@$(CH_2)_3$−urea−thiazole (d), and Fe_3O_4@SiO_2@$(CH_2)_3$−urea−thiazole sulfonic acid chloride (e).

2. RESULT AND DISCUSSION

Development of the knowledge of catalysts and catalytic systems are our major interest. For many years, the application of catalysts had been an attractive matter for researchers all over the world. Therefore, we decided to develop our knowledge on the design, synthesis, and application of new catalysts for synthesis target molecules which are proceeded via an anomeric-based oxidation mechanism.

https://dx.doi.org/10.1021/acsomega.9b03277
ACS Omega 2020, 5, 3207−3217

2.1. Characterization of Novel Catalyst. First, by applying proper techniques including Fourier transform infrared (FT-IR), energy-dispersive X-ray (EDX), elemental mapping, thermo gravimetric analysis/differential thermal analysis (TGA/DTA), scanning electron microscopy (SEM), transmission electron microscopy (TEM), and vibrating sample magnetometry (VSM), the structure and successful formation of Fe_3O_4@SiO_2@$(CH_2)_3$−urea−thiazole sulfonic acid chloride were confirmed. The outcome of all applied analysis was discussed below in detail.

In a comparative manner, FT-IR spectra of each stage of the preparation pathway of the catalyst from urea-based ligand (a), Fe_3O_4 (b), Fe_3O_4@SiO_2 (c), Fe_3O_4@SiO_2@$(CH_2)_3$−urea−thiazole (d) and Fe_3O_4@SiO_2@$(CH_2)_3$−urea−thiazole sulfonic acid chloride (e) as a target structure were investigated (Figure 1). The FT-IR spectrum of the desired catalyst represents all predictable functional groups at their related positions. Broad peak from about 2700−3700 cm^{-1} as the fingerprint confirms the existence of acidic OH and NH functional groups. Also, the C═O group in the urea moiety verified by a peak at 1720 cm^{-1}. A peak observed at 1225 cm^{-1} is related to S═O groups. Also, related bands to Fe−O and Si−O functional groups appeared at around 636 and 1096 cm^{-1}, respectively.[63]

For elemental analysis and chemical characterization of the Fe_3O_4@SiO_2@$(CH_2)_3$−urea−thiazole sulfonic acid chloride, EDX analysis was used. The obtained data, as shown in Figure 2, approved all desired atoms, namely, iron, oxygen, silicium,

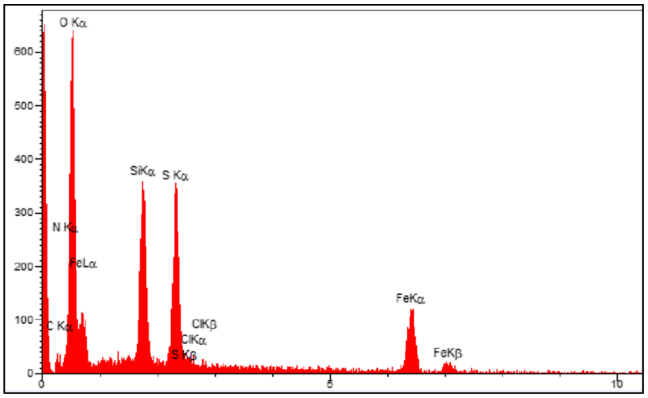

Figure 2. EDX analysis of Fe_3O_4@SiO_2@$(CH_2)_3$−urea−thiazole sulfonic acid chloride.

carbon, nitrogen, sulfur, and chlorine within the structure of the prepared catalyst. Also, these observations are verified by the achieved data from the elemental mapping analysis as indicated in Figure 3. Therefore, it can be concluded that the functionalization of the surface of Fe_3O_4 nanoparticles is succeeded.

In another exploration, surface topography of the novel prepared nanomagnetic catalyst through scanning the surface by SEM was investigated (Figure 4). The attained SEM micrographs verified the spherical shape of the prepared structure which consists of particles in the domain of the nanometer scale. Also, the obtained images from TEM confirmed the nanosized structure of the prepared catalyst (Figure 5).

The obtained TG and DTG analysis curves of the prepared catalyst were depicted in Figure 6. These curves predict high thermal stability for the presented novel-synthesized nanomagnetic catalyst and guarantees its application at operational elevated temperatures.

Using VSM, the magnetic behavior of the prepared nanomagnetic catalyst and its related intermediates including Fe_3O_4@SiO_2 and Fe_3O_4@SiO_2@$(CH_2)_3$−urea−thiazole are depicted in Figure 7. These data revealed that the insertion of each layer to the surface of Fe_3O_4 nanoparticles reduced its magnetic properties and confirmed the successful formation of the desired catalyst.

2.2. Catalytic Application of Novel Ionically Tagged Magnetic Nanoparticles with a Urea Linker for the Preparation of 2-Aryl-quinoline-4-carboxylic Acids. After the synthesis and identification of the novel Fe_3O_4@SiO_2@$(CH_2)_3$−urea−thiazole sulfonic acid chloride, its catalytic behavior was investigated in the preparation of 2-aryl-quinoline-4-carboxylic acid derivatives. To attain the optimal reaction parameters, the reaction of 4-methyl benzaldehyde, pyruvic acid, and 1-naphthylamine was considered as the model reaction. Upon the model reaction, the effect of reaction temperature, catalyst loading, and solvent was checked out. On the basis of our achieved experimental results, using 10 mg of the Fe_3O_4@SiO_2@$(CH_2)_3$−urea−thiazole sulfonic acid chloride at 80 °C under solvent-free conditions supplied the best results. Elevating the operational reaction temperature and increasing the amount of the catalyst did not lead to more favorable results. All obtained data are summarized in Table 1.

Also, we performed the model reaction in the presence of related intermediates of Fe_3O_4@SiO_2@$(CH_2)_3$−urea−thiazole sulfonic acid chloride at 80 °C under solvent-free conditions for 30 min. The achieved data as inserted in Table 2 shows no satisfactory results compared with Fe_3O_4@SiO_2@$(CH_2)_3$−urea−thiazole sulfonic acid chloride.

Afterward, we focus on the generality and scope of the presented protocol. The test was developed using different aromatic aldehydes such as aldehydes bearing electron-releasing or withdrawing substituents and halogens on their aromatic ring. The obtained experimental data are included in the Table 3. All desired 2-aryl-quinoline-4-carboxylic acid derivatives were furnished in short reaction times with high yields. Also, in order to expand the generality and scope of the reaction, we tried to use aniline instead of 1-naphthylamine to prepare the desired molecule **2a**, but these conditions lead to the formation of the mixture of products; the reaction was sluggish (Scheme 7).

Also, we explored the recovery and reusability of Fe_3O_4@SiO_2@$(CH_2)_3$−urea−thiazole sulfonic acid chloride in a model reaction for the synthesis of target molecule **1b** under the obtained optimized reaction parameters for 30 min. After each individual run, hot ethanol was added to the reaction mixture. Fe_3O_4@SiO_2@$(CH_2)_3$−urea−thiazole sulfonic acid chloride was insoluble in the solvent, and thus it can be easily separated from the reaction mixture by applying a simple external magnet. Then, the recovered catalyst washed well with ethanol, dried, and preserved for next run. Fortunately, as illustrated in Figure 8, Fe_3O_4@SiO_2@$(CH_2)_3$−urea−thiazole sulfonic acid chloride displayed elegant recovery and reusability in model reaction.

Also, we suggested a plausible mechanistic pathway for the construction of desired molecules **1a** as model via an anomeric based oxidation in the presence of Fe_3O_4@SiO_2@$(CH_2)_3$−urea−thiazole sulfonic acid chloride (Scheme 8). Initially, naphthylamine acts as a nucleophile and attacks the catalytic

https://dx.doi.org/10.1021/acsomega.9b03277
ACS Omega 2020, 5, 3207−3217

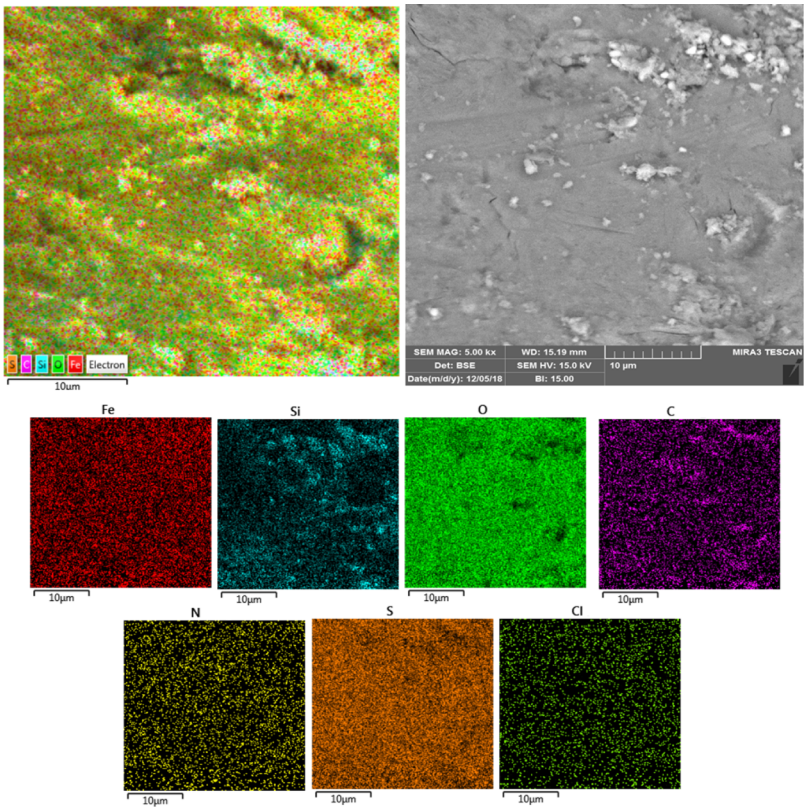

Figure 3. Elemental mapping analysis of $Fe_3O_4@SiO_2@(CH_2)_3$–urea–thiazole sulfonic acid chloride.

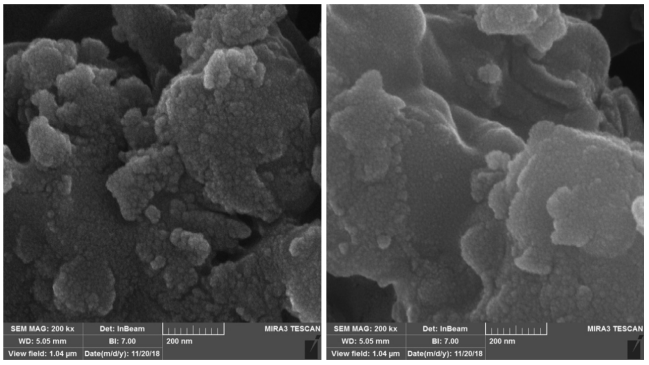

Figure 4. SEM micrographs of the $Fe_3O_4@SiO_2@(CH_2)_3$–urea–thiazole sulfonic acid chloride.

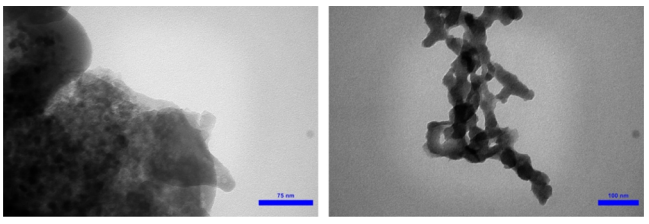

Figure 5. TEM images of the $Fe_3O_4@SiO_2@(CH_2)_3$–urea–thiazole sulfonic acid chloride.

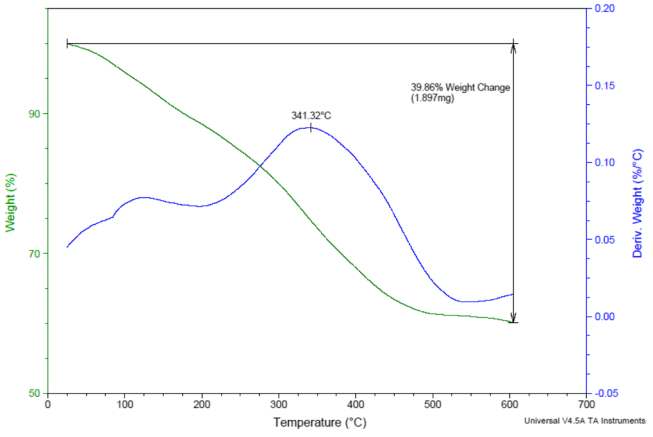

Figure 6. TG and DTG analysis curves of $Fe_3O_4@SiO_2@(CH_2)_3$–urea–thiazole sulfonic acid chloride.

activated benzaldehyde which is converted to imine intermediate **I**. In the next step, enol form of pyruvic acid **II**, attacks the imine intermediate **I** which leads to the formation of intermediate **III**. Then, in the presence of the catalyst, through cyclization and dehydration processes, intermediate **III** is converted to the intermediate **V**. In the final step of the presented mechanism, in the intermediate **V**, lone pair electrons of the nitrogen atom and also C–C double bonds interact with a vacant antibonding orbital of the C–H bond ($n_N \rightarrow \sigma^*_{C-H}$ and $\pi_{C=C} \rightarrow \sigma^*_{C-H}$) and weaken it, which facilitates hydride transfer. This phenomenon leads to the aromatization of intermediate **V**, furnishing of the desired molecule **1a,** and recovery of the catalyst.

3. CONCLUSIONS

To sum it up, this exploration deals with the design and synthesis of novel ionically tagged magnetic nanoparticles bearing urea linker, namely, $Fe_3O_4@SiO_2@(CH_2)_3$–urea–thiazole sulfonic acid chloride. The mentioned catalyst was fully characterized using various techniques. The catalytic

https://dx.doi.org/10.1021/acsomega.9b03277
ACS Omega 2020, 5, 3207–3217

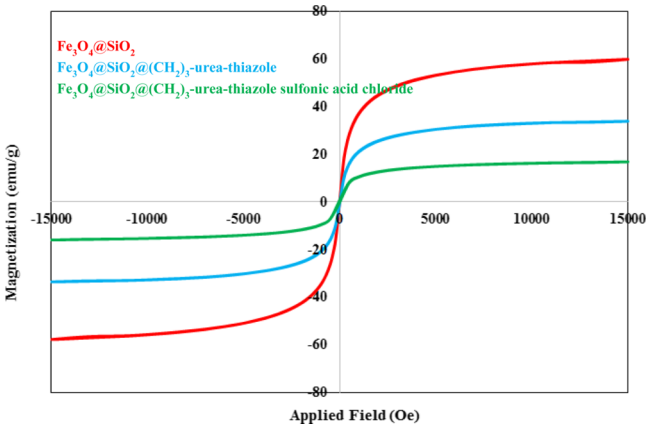

Figure 7. VSM curves of Fe_3O_4@SiO_2, Fe_3O_4@SiO_2@$(CH_2)_3$–urea–thiazole and Fe_3O_4@SiO_2@$(CH_2)_3$–urea–thiazole sulfonic acid chloride.

Table 1. Optimization of Reaction Conditions upon the Synthesis of Molecule 1a in the Presence of Fe_3O_4@SiO_2@$(CH_2)_3$–Urea–Thiazole Sulfonic Acid Chloride as a Novel Catalyst[a]

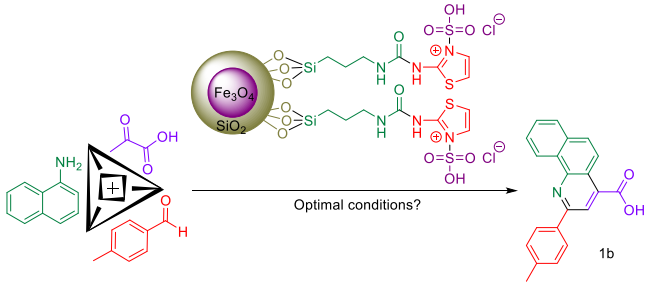

entry	solvent	temperature (°C)	catalyst (mg)	time (min)	yield (%)[b]
1		100	10	40	80
2[c]		80	10	30	85
3		70	10	50	75
4		80	6	60	73
5		80	14	45	75
6		80		90	60
7	H_2O	reflux	10	90	75
8	EtOH	reflux	10	90	85
9	EtOAc	reflux	10	120	65
10	THF	reflux	10	120	60
11	CH_3CN	reflux	10	120	60
12	*n*-hexane	reflux	10	120	55

[a]Reaction conditions: 4-methylbenzaldehyde (1 mmol, 0.120 g), pyruvic acid (1 mmol, 0.088 g), and 1-naphthylamine (1 mmol, 0.143 g). [b]Isolated yields. [c]Data for the model reaction under air, nitrogen and argon atmosphere are similar.

capability of the presented catalyst on the synthesis of 2-aryl-quinoline-4-carboxylic acid derivatives via anomeric based oxidation was successfully investigated. All desired molecules were obtained in short reaction times with high yields. The described catalyst shows elegant recovery and reusing potential in the studied MCR.

4. EXPERIMENTAL SECTION

4.1. General Procedure for the Synthesis of the Urea-Based Ligand. At first, urea-based ligand was prepared by the reaction of triethoxy(3-isocyanatopropyl)silane (5 mmol, 1.237 g) and 2-aminothiazole (5 mmol, 0.501 g) under solvent-free conditions at 60 °C for 6 h. Afterward, the obtained product was washed with a mixture of *n*-hexane and dichloromethane (3 × 10 mL) to afford the desired urea-based ligand (Scheme 5).

Table 2. Screening the Model Reaction in the Presence of the Desired Catalyst and Its Related Intermediates[a]

entry	catalyst	yield (%)[b]
1	Fe_3O_4	65
2	Fe_3O_4@SiO_2	60
3	Fe_3O_4@SiO_2@$(CH_2)_3$–urea–thiazole	70
4	Fe_3O_4@SiO_2@$(CH_2)_3$–urea–thiazole sulfonic acid chloride	85

[a]Reaction conditions:: 4-methylbenzaldehyde (1 mmol, 0.120 g), pyruvic acid (1 mmol, 0.088 g), and 1-naphthylamine (1 mmol, 0.143 g), catalyst: 10 mg. [b]Isolated yields.

Table 3. Catalytic Synthesis of 2-Aryl-quinoline-4-carboxylic Acid Derivatives in the Presence of a Catalytic Amount of Fe_3O_4@SiO_2@$(CH_2)_3$–Urea–Thiazole Sulfonic Acid Chloride[a]

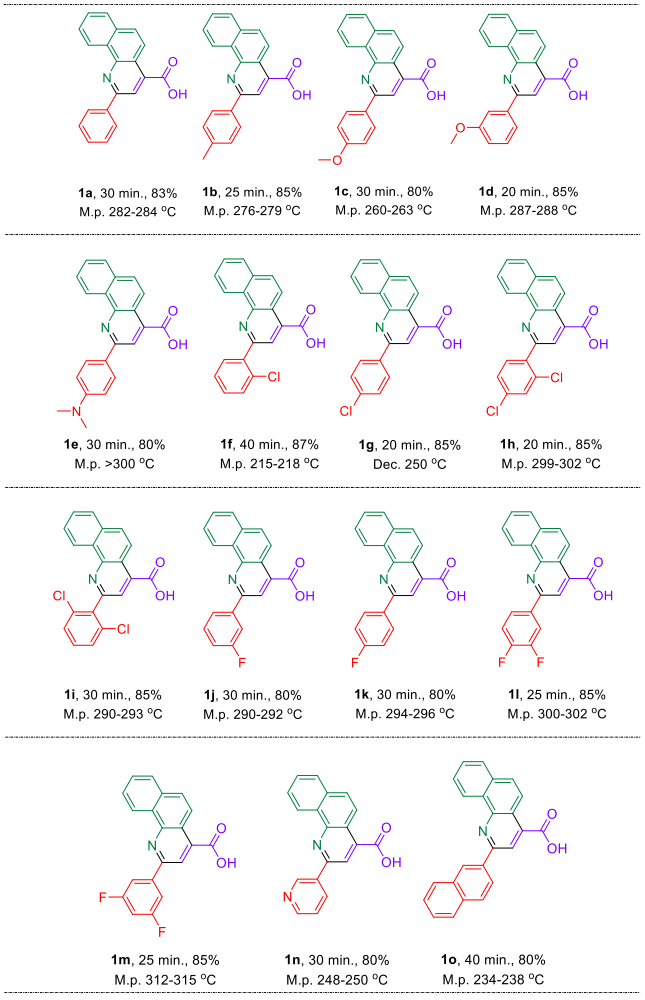

[a]Reaction conditions: arylaldehyde (1 mmol), pyruvic acid (1 mmol, 0.088 g), and 1-naphthylamine (1 mmol, 0.143 g), optimal reaction conditions, isolated yields.

https://dx.doi.org/10.1021/acsomega.9b03277
ACS Omega 2020, 5, 3207−3217

Scheme 7. Investigation of the Scope and Generality of the Reaction by Using Different Amines

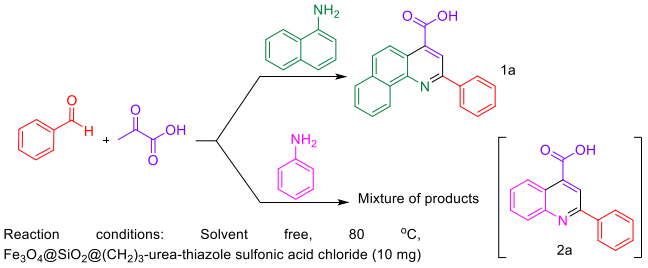

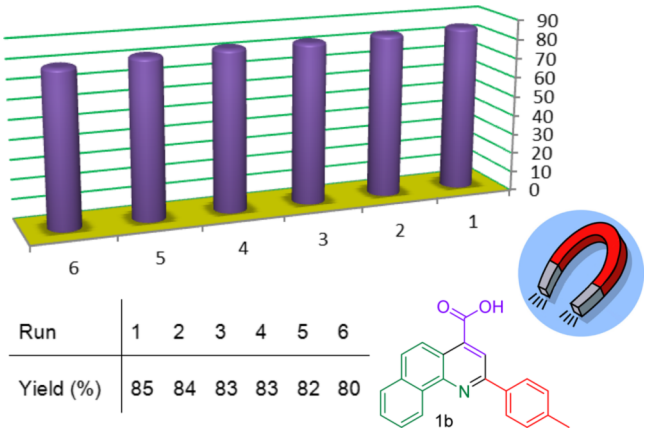

Run	1	2	3	4	5	6
Yield (%)	85	84	83	83	82	80

Figure 8. Successful reusing test of Fe_3O_4@SiO_2@$(CH_2)_3$–urea–thiazole sulfonic acid chloride at the synthesis of target molecules **1b**.

4.2. General Procedure for the Synthesis of Fe_3O_4@SiO_2@$(CH_2)_3$–Urea–Thiazole Sulfonic Acid Chloride. Initially, Fe_3O_4 nanoparticles were prepared in a similar manner to the previously reported procedure.[64] In the next step, Fe_3O_4@SiO_2 was prepared through the reaction of Fe_3O_4 nanoparticles with tetraethyl orthosilicate (TEOS). Afterward, the obtained Fe_3O_4@SiO_2 (1 g) was functionalized by the reaction with urea-based ligand (2 mmol, 0.695 g) under refluxing toluene. In the next step, the obtained Fe_3O_4@SiO_2@$(CH_2)_3$–urea–thiazole was subjected to the reaction with chlorosulfuric acid (21.928 mmol, 0.233 g) in dichloromethane, as a solvent, at room temperature. In the final step, Fe_3O_4@SiO_2@$(CH_2)_3$–urea–thiazole sulfonic acid chloride was washed thoroughly with [dichloromethane (3 × 15 mL)] and dried (Scheme 5).

4.3. General Procedure for the Synthesis of 2-Aryl-quinoline-4-carboxylic Acid Derivatives in the Presence of Fe_3O_4@SiO_2@$(CH_2)_3$–Urea–Thiazole Sulfonic Acid Chloride. In a round-bottomed flask, a mixture of arylaldehyde derivatives (1 mmol), pyruvic acid (1 mmol, 0.088 g), 1-naphthylamine (1 mmol, 0.143 g), and Fe_3O_4@SiO_2@$(CH_2)_3$–urea–thiazole sulfonic acid chloride (10 mg) was stirred vigorously at 80 °C under solvent-free conditions for appropriate times (Table 2). The reaction progress and completion were monitored by using the thin-layer chromatography technique with *n*-hexane and ethyl acetate (4:6). After reaction completion, hot ethanol was added to the mixture to dissolve the unreacted starting materials and products. Then, Fe_3O_4@SiO_2@$(CH_2)_3$–urea–thiazole sulfonic acid chloride was easily separated by using an external magnet. Finally, recrystallization using ethanol gives desired 2-aryl-quinoline-4-carboxylic acid derivatives in high yields.

4.4. General Procedure for the Recycling and Reusing Test of Fe_3O_4@SiO_2@$(CH_2)_3$–Urea–Thiazole Sulfonic Acid Chloride for the Synthesis of Molecule 1b. In

Scheme 8. Reasonable Mechanistic Pathway for the Synthesis of Molecule 1a

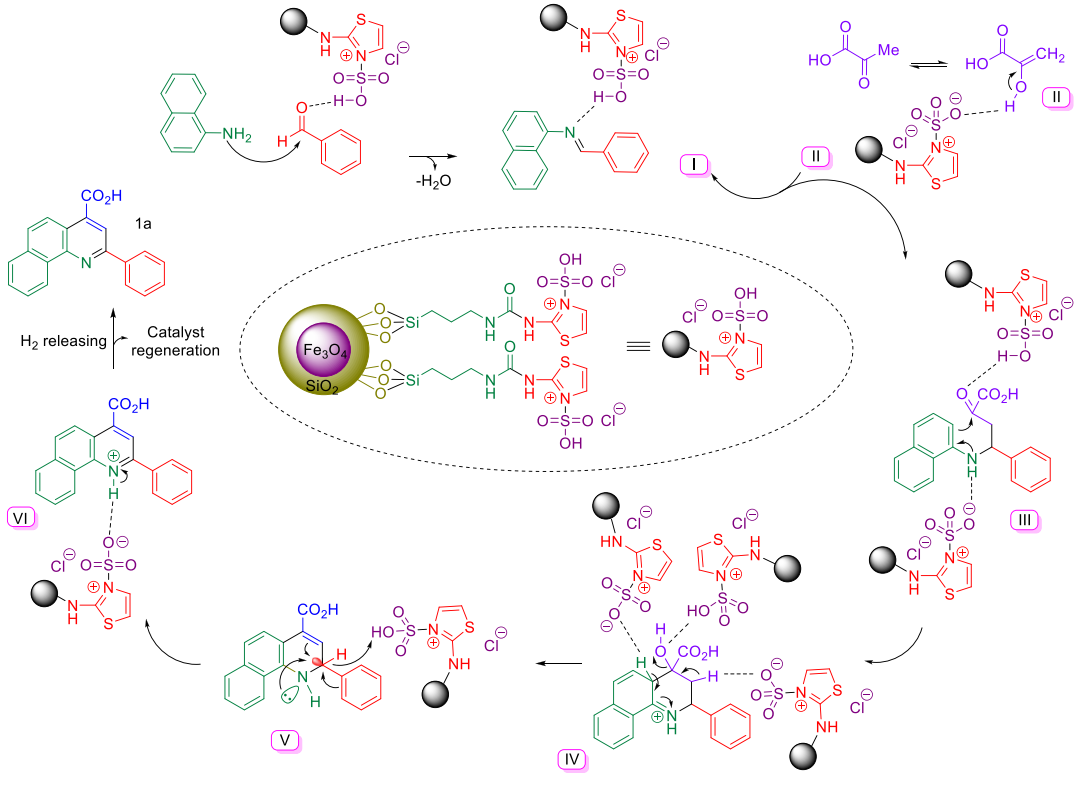

https://dx.doi.org/10.1021/acsomega.9b03277
ACS Omega 2020, 5, 3207−3217

order to explore the recovering and reusability of Fe_3O_4@SiO_2@$(CH_2)_3$−urea−thiazole sulfonic acid chloride, synthesis of target molecule **1b** was selected as the model reaction. The model reaction was performed under the obtained optimized reaction parameters for 30 min. After each individual run, hot ethanol was added to the reaction mixture. Fe_3O_4@SiO_2@$(CH_2)_3$−urea−thiazole sulfonic acid chloride was insoluble in the solvent, thus it can be easily separated from the reaction mixture by applying a simple external magnet. Then, the recovered catalyst was washed well with ethanol, dried, and preserved for the next run. The obtained experimental data, as illustrated in the Figure 8, confirmed elegant recovering and reusability of the Fe_3O_4@SiO_2@$(CH_2)_3$−urea−thiazole sulfonic acid chloride in the model reaction.

4.5. Selected Spectral Data. *4.5.1. 1-(Thiazol-2-yl)-3-(3-(triethoxysilyl)propyl)urea (Urea Based Ligand).* ^{1}H NMR (400 MHz, DMSO, δ, ppm): 10.34 (s, 1H, NH), 7.31 (d, 1H, J = 3 Hz, Thiazole ring), 7.00 (d, 1H, J = 3 Hz, thiazole ring), 6.58 (s, 1H, NH), 3.76 (q, 6H, J = 6 Hz, CH_2), 3.13 (t, 2H, J = 6 Hz, CH_2), 1.51 (q, 2H, J = 6 Hz, CH_2), 1.16 (t, 9H, J = 6 Hz, CH_3), 0.56 (t, 9H, J = 6 Hz, CH_2). ^{13}C NMR (100 MHz, DMSO, δ, ppm): 160.6, 154.3, 137.7, 112.1, 58.2, 42.3, 23.6, 18.6, 7.6.

*4.5.2. 2-Phenylbenzo[h]quinoline-4-carboxylic Acid (**1a**).* mp 282−284 °C. FT-IR (KBr, ν, cm^{-1}): 3444, 3062, 1705, 1582, 1256, 830.

^{1}H NMR (400 MHz, DMSO, δ, ppm): 13.94 (br s, 1H, OH), 9.42 (s, 1H, aromatic), 8.56 (d, 2H, J = 16 Hz, aromatic), 8.48 (s, 2H, aromatic), 8.08 (s, 2H, aromatic), 7.84 (s, 2H, aromatic), 7.61 (d, 3H, J = 20 Hz, aromatic).

^{13}C NMR (100 MHz, DMSO, δ, ppm): 168.4, 154.8, 146.7, 138.7, 138.5, 133.6, 131.3, 130.4, 129.6, 129.4, 129.1, 128.4, 128.0, 127.6, 124.9, 122.8, 122.3, 119.3.

*4.5.3. 2-(p-Tolyl)benzo[h]quinoline-4-carboxylic Acid (**1b**).* mp 276−279 °C. FT-IR (KBr, ν, cm^{-1}): 3063, 2923, 1697, 1582, 1255, 829.

^{1}H NMR (400 MHz, DMSO, δ, ppm): 13.88 (br s, 1H, OH), 9.41 (s, 1H, aromatic), 8.53 (d, 2H, J = 12 Hz, aromatic), 8.37 (d, 2H, J = 4 Hz, aromatic), 8.08−8.04 (m, 2H, aromatic), 7.84 (s, 2H, aromatic), 7.45 (s, 2H, aromatic), 2.44 (s, 3H, Me).

^{13}C NMR (100 MHz, DMSO, δ, ppm): 168.4, 154.8, 146.7, 140.2, 135.8, 133.6, 131.2, 130.2, 129.4, 128.9, 128.4, 127.9, 127.5, 124.9, 122.8, 122.1, 119.0, 21.4.

*4.5.4. 2-(4-Methoxyphenyl)benzo[h]quinoline-4-carboxylic Acid (**1c**).* mp 260−263 °C. FT-IR (KBr, ν, cm^{-1}): 3447, 3067, 2960, 2925, 1705, 1583, 1267, 826.

^{1}H NMR (400 MHz, DMSO, δ, ppm): 14.09 (br s, 1H, OH), 9.39 (s, 1H, aromatic), 8.51−8.44 (m, 4H, aromatic), 8.05 (d, 2H, J = 20 Hz, aromatic), 7.83, (s, 2H, aromatic), 7.17 (s, 2H, aromatic), 3.89 (s, 3H, OMe).

^{13}C NMR (100 MHz, DMSO, δ, ppm): 168.1, 160.8, 154.1, 146.1, 133.1, 131.8, 130.7, 130.6, 128.6, 128.0, 127.9, 127.3, 124.4, 122.5, 121.3, 118.1, 114.4, 55.3.

*4.5.5. 2-(3-Methoxyphenyl)benzo[h]quinoline-4-carboxylic Acid (**1d**).* mp 287−288 °C. FT-IR (KBr, ν, cm^{-1}): 3446, 3061, 2972, 1704, 1583, 1278, 751.

^{1}H NMR (400 MHz, DMSO, δ, ppm): 14.00 (br s, 1H, OH), 9.38 (d, 1H, J = 8 Hz, aromatic), 8.53 (d, 1H, J = 8 Hz, aromatic), 8.46 (s, 1H, aromatic), 8.07−8.02 (m, 2H, aromatic), 7.99−7.76 (m, 4H, aromatic), 7.12 (d, 1H, J = 8 Hz, aromatic), 3.884 (s, 3H, Me).

^{13}C NMR (100 MHz, DMSO, δ, ppm): 167.9, 154.2, 149.6, 146.9, 146.1, 137.7, 133.1, 130.7, 130.7, 128.7, 128.0, 127.9, 127.2, 124.3, 122.4, 121.3, 118.5, 118.3, 113.9, 112.2, 55.6.

*4.5.6. 2-(4-(Dimethylamino)phenyl)benzo[h]quinoline-4-carboxylic Acid (**1e**).* mp > 300 °C. FT-IR (KBr, ν, cm^{-1}): 3431, 3041, 2917, 1688, 1610, 1580, 1262, 821.

^{1}H NMR (400 MHz, DMSO, δ, ppm): 13.91 (br s, 1H, OH), 9.38 (s, 1H, aromatic), 8.43−8.33 (m, 4H, aromatic), 8.00 (d, 2H, J = 32 Hz, aromatic), 7.80 (s, 2H, aromatic), 6.92 (s, 2H, aromatic), 3.05 (s, 6H, $N(Me)_2$).

^{13}C NMR (100 MHz, DMSO, δ, ppm): 168.0, 151.4, 139.7, 133.9, 133.1, 130.7, 128.6, 128.0, 127.8, 127.2, 127.1, 125.2, 124.4, 120.7, 117.6, 112.0, 40.0.

*4.5.7. 2-(2-Chlorophenyl)benzo[h]quinoline-4-carboxylic Acid (**1f**).* mp 215−218 °C. FT-IR (KBr, ν, cm^{-1}): 3443, 3065, 1707, 1583, 1260, 743.

^{1}H NMR (400 MHz, DMSO, δ, ppm): 13.71 (br s, 1H, OH), 9.24 (s, 1H, aromatic), 8.62 (d, 1H, J = 12 Hz, aromatic), 8.28 (s, 1H, aromatic), 8.11 (d, 2H, J = 8 Hz, aromatic), 7.88 (d, 1H, J = 4 Hz, aromatic), 7.81 (d, 2H, J = 4 Hz, aromatic), 7.70 (t, 1H, J = 4 Hz, aromatic), 7.59 (d, 2H, J = 4 Hz, aromatic).

^{13}C NMR (100 MHz, DMSO, δ, ppm): 167.8, 154.7, 146.2, 138.4, 137.8, 132.9, 132.1, 132.1, 131.3, 130.6, 130.6, 130.2, 130.2, 129.1, 128.9, 127.9, 127.7, 127.5, 124.3, 122.8, 122.4, 121.8.

*4.5.8. 2-(4-Chlorophenyl)benzo[h]quinoline-4-carboxylic Acid (**1g**).* mp 250 °C dec. FT-IR (KBr, ν, cm^{-1}): 3062, 1698, 1581, 1254, 830.

^{1}H NMR (400 MHz, DMSO, δ, ppm): 13.94 (br s, 1H, OH), 9.40 (d, 1H, J = 8 Hz, aromatic), 8.59−8.50 (m, 4H, aromatic), 8.08 (t, 2H, J = 8 Hz, aromatic), 7.84 (t, 2H, J = 4 Hz, aromatic), 7.68 (d, 2H, J = 8 Hz, aromatic).

^{13}C NMR (100 MHz, DMSO, δ, ppm): 167.8, 153.1, 153.0, 146.2, 136.8, 134.8, 133.1, 130.7, 129.7, 129.3, 129.1, 129.0, 128.9, 128.8, 128.0, 127.5, 124.4, 122.3, 122.0, 118.7.

*4.5.9. 2-(2,4-Dichlorophenyl)benzo[h]quinoline-4-carboxylic Acid (**1h**).* mp 299−302 °C. FT-IR (KBr, ν, cm^{-1}): 3448, 3064, 1704, 1585, 1261, 834.

^{1}H NMR (400 MHz, DMSO, δ, ppm): 14.12 (br s, 1H, OH), 9.23 (d, 1H, J = 8 Hz, aromatic), 8.62 (d, 2H, J = 8 Hz, aromatic), 8.32 (s, 1H, aromatic), 8.12 (t, 2H, J = 8 Hz, aromatic), 7.94−7.87 (m, 2H, aromatic), 7.83−7.81 (m, 1H, aromatic), 7.68 (d, 1H, J = 8 Hz, aromatic).

^{13}C NMR (100 MHz, DMSO, δ, ppm): 167.5, 153.6, 146.2, 137.2, 137.1, 134.5, 133.4, 132.9, 132.4, 130.5, 129.6, 129.4, 129.0, 127.9, 127.9, 127.6, 124.3, 122.9, 122.2, 122.0.

*4.5.10. 2-(2,6-Dichlorophenyl)benzo[h]quinoline-4-carboxylic Acid (**1i**).* mp 290−293 °C. FT-IR (KBr, ν, cm^{-1}): 3448, 3064, 1704, 1585, 1261, 834.

^{1}H NMR (400 MHz, DMSO, δ, ppm): 14.20 (br s, 1H, OH), 9.40 (d, 1H, J = 8 Hz, aromatic), 8.58 (s, 1H, aromatic), 8.54 (d, 2H, J = 8 Hz, aromatic), 8.45 (d, 2H, J = 8 Hz, aromatic), 8.08 (t, 2H, J = 8 Hz, aromatic), 7.87−7.81 (m, 2H, aromatic).

^{13}C NMR (100 MHz, DMSO, δ, ppm): 167.5, 153.6, 146.2, 137.2, 137.1, 134.5, 133.4, 132.9, 132.4, 130.5, 129.6, 129.4, 129.0, 127.9, 127.9, 127.6, 124.3, 122.9, 122.2, 122.0.

*4.5.11. 2-(3-Fluorophenyl)benzo[h]quinoline-4-carboxylic Acid (**1j**).* mp 290−292 °C. FT-IR (KBr, ν, cm^{-1}): 3078, 1694, 1590, 1259, 833.

^{1}H NMR (400 MHz, DMSO, δ, ppm): 13.99 (br s, 1H, OH), 9.40 (d, 1H, J = 8 Hz, aromatic), 8.60 (s, 1H, aromatic),

https://dx.doi.org/10.1021/acsomega.9b03277
ACS Omega 2020, 5, 3207−3217

8.51 (d, 1H, J = 8 Hz, aromatic), 8.32−8.28 (t, 2H, J = 8 Hz, aromatic), 8.09−8.05 (t, 2H, J = 8 Hz, aromatic), 7.87−7.81 (m, 2H, aromatic), 7.69−7.63 (m, 1H, aromatic), 7.40 (t, 1H, J = 8 Hz, aromatic).

^{13}C NMR (100 MHz, DMSO, δ, ppm): 167.9, 167.8, 164.1, 161.6, 152.9, 152.8, 146.1, 140.6, 140.5, 138.6, 133.1, 131.1, 131.0, 130.6, 129.1, 129.0, 127.9, 127.6, 124.5, 123.2, 122.3, 122.1, 118.9, 116.7, 116.5, 113.8, 113.6.

*4.5.12. 2-(3,4-Difluorophenyl)benzo[h]quinoline-4-carboxylic Acid (**1l**).* mp 300−302 °C. FT-IR (KBr, ν, cm^{-1}): 3414, 3053, 1701, 1582, 1258, 829.

^{1}H NMR (400 MHz, DMSO, δ, ppm): 13.61 (br s, 1H, OH), 9.38 (d, 1H, J = 8 Hz, aromatic), 8.55−8.31 (m, 4H, aromatic), 8.12−7.97 (m, 2H, aromatic), 7.83−7.80 (m, 2H, aromatic), 7.68−7.25 (m, 2H, aromatic).

^{13}C NMR (100 MHz, DMSO, δ, ppm): 168.0, 152.0, 151.7, 151.2, 150.4, 149.4, 149.3, 148.8, 146.0, 144.4, 139.5, 135.7, 133.1, 133.1, 130.6, 130.2, 129.9, 128.9, 128.8, 128.8, 128.0, 127.9, 127.7, 127.6, 127.5, 127.3, 127.1, 124.5, 124.1, 122.5, 122.4, 122.0, 118.4, 118.1, 117.9, 116.2, 116.0.

*4.5.13. 2-(3,5-Difluorophenyl)benzo[h]quinoline-4-carboxylic Acid (**1m**).* mp 312−315 °C. FT-IR (KBr, ν, cm^{-1}): 3454, 3064, 1695, 1599, 1265, 833.

^{1}H NMR (400 MHz, DMSO, δ, ppm): 13.96 (br s, 1H, OH), 9.41 (s, 1H, aromatic), 8.64 (s, 1H, aromatic), 8.50 (d, 1H, J = 12 Hz, aromatic), 8.22 (d, 2H, J = 8 Hz, aromatic), 8.09 (d, 2H, J = 8 Hz, aromatic), 7.86 (d, 2H, aromatic), 7.46 (t, 1H, aromatic).

^{13}C NMR (100 MHz, DMSO, δ, ppm): 167.8, 164.3, 161.9, 146.1, 133.1, 130.6, 129.4, 129.4, 129.1, 128.0, 127.7, 124.6, 122.4, 122.2, 122.2, 119.0, 119.0, 110.4, 110.1, 105.4, 105.2, 104.9.

*4.5.14. 2-(Pyridin-3-yl)benzo[h]quinoline-4-carboxylic Acid (**1n**).* mp 248−250 °C. FT-IR (KBr, ν, cm^{-1}): 3436, 3049, 1713, 1582, 1266, 836.

^{1}H NMR (400 MHz, DMSO, δ, ppm): 14.21 (br s, 1H, OH), 9.64 (s, 1H, aromatic), 9.43 (s, 1H, aromatic), 8.79 (d, 2H, J = 28 Hz, aromatic), 8.65 (s, 1H, aromatic), 8.53 (d, 1H, J = 8 Hz, aromatic), 8.10 (s, 2H, aromatic), 7.85 (s, 2H, aromatic), 7.65 (s, 1H, aromatic).

^{13}C NMR (100 MHz, DMSO, δ, ppm): 167.8, 152.3, 150.5, 148.3, 146.3, 138.8, 134.7, 133.6, 133.1, 130.6, 129.1, 128.0, 127.6, 124.5, 124.0, 122.3, 122.1, 118.9.

*4.5.15. 2-(Naphthalen-2-yl)benzo[h]quinoline-4-carboxylic Acid (**1o**).* mp 234−238 °C. FT-IR (KBr, ν, cm^{-1}): 3446, 3050, 1694, 1584, 1258, 753.

^{1}H NMR (400 MHz, DMSO, δ, ppm): 13.93 (br s, 1H, OH), 9.51 (d, 1H, J = 8 Hz, aromatic), 9.04 (s, 1H, aromatic), 8.77 (s, 1H, aromatic), 8.71 (d, 1H, J = 8 Hz, aromatic), 8.57 (d, 1H, J = 8 Hz, aromatic), 8.23−8.16 (m, 2H, aromatic), 8.11−8.04 (m, 3H, aromatic), 7.86 (q, 2H, J = 8 Hz, aromatic), 7.64−7.62 (m, 2H, aromatic).

^{13}C NMR (100 MHz, DMSO, δ, ppm): 168.0, 154.2, 146.3, 138.5, 135.4, 133.6, 133.2, 133.1, 130.8, 128.9, 128.6, 128.0, 127.6, 127.5, 127.2, 126.8, 126.6, 124.6, 124.5, 122.4, 121.9, 119.0.

■ ASSOCIATED CONTENT

Supporting Information

The Supporting Information is available free of charge at https://pubs.acs.org/doi/10.1021/acsomega.9b03277.

Copies of FT-IR, ^{1}H NMR, and ^{13}C NMR spectra of compounds (PDF)

■ AUTHOR INFORMATION

Corresponding Authors

Meysam Yarie − *Department of Organic Chemistry, Faculty of Chemistry, Bu-Ali Sina University, Hamedan 6516738695, Iran;* orcid.org/0000-0002-7129-0776; Phone: +98 8138282807; Email: myari.5266@gmail.com; Fax: +98 8138257407

Mohammad Ali Zolfigol − *Department of Organic Chemistry, Faculty of Chemistry, Bu-Ali Sina University, Hamedan 6516738695, Iran;* orcid.org/0000-0002-4970-8646; Email: zolfi@basu.ac.ir, mzolfigol@yahoo.com

Avat Arman Taherpour − *Department of Organic Chemistry, Razi University, Kermanshah 6714414971, Iran; Medical Biology Research Center, Kermanshah University of Medical Sciences, Kermanshah 6715847141, Iran;* Email: avatarman.taherpour@gmail.com

Authors

Parvin Ghasemi − *Department of Organic Chemistry, Razi University, Kermanshah 6714414971, Iran*

Morteza Torabi − *Department of Organic Chemistry, Faculty of Chemistry, Bu-Ali Sina University, Hamedan 6516738695, Iran*

Complete contact information is available at: https://pubs.acs.org/10.1021/acsomega.9b03277

Notes

The authors declare no competing financial interest.

■ ACKNOWLEDGMENTS

We thank the Bu-Ali Sina University, Razi University, National Elites Foundation and Iran National Science Foundation (INSF) (grant number: 98001912) for financial support to our research group.

■ REFERENCES

(1) Zablotskaya, A.; Segal, I.; Geronikaki, A.; Shestakova, I.; Nikolajeva, V.; Makarenkova, G. N-Heterocyclic choline analogues based on 1,2,3,4-tetrahydro(iso)quinoline scaffold with anticancer and anti-infective dual action. *Pharmacol. Rep.* **2017**, *69*, 575−581.

(2) Sun, N.; Du, R.-L.; Zheng, Y.-Y.; Huang, B.-H.; Guo, Q.; Zhang, R.-F.; Wong, K.-Y.; Lu, Y.-J. Antibacterial activity of N-methylbenzofuro [3,2-b] quinoline and N-methylbenzoindolo [3,2-b]-quinoline derivatives and study of their mode of action. *Eur. J. Med. Chem.* **2017**, *135*, 1−11.

(3) Nathubhai, A.; Haikarainen, T.; Koivunen, J.; Murthy, S.; Koumanov, F.; Lloyd, M. D.; Holman, G. D.; Pihlajaniemi, T.; Tosh, D.; Lehtiö, L.; Threadgill, M. D. Threadgill, Highly potent and isoform selective dual site binding Tankyrase/Wnt signaling inhibitors that increase cellular glucose uptake and have antiproliferative activity. *J. Med. Chem.* **2017**, *60*, 814−820.

(4) Murugavel, S.; Jacob Prasanna Stephen, C. S.; Subashini, R.; AnanthaKrishnan, D. Synthesis, structural elucidation, antioxidant, CT-DNA binding and molecular docking studies of novel chloroquinoline derivatives: Promising antioxidant and anti-diabetic agents. *J. Photochem. Photobiol., B* **2017**, *173*, 216−230.

(5) Nainwal, L. M.; Tasneem, S.; Akhtar, W.; Verma, G.; Khan, M. F.; Parvez, S.; Shaquiquzzaman, M.; Akhter, M.; Alam, M. M. Green recipes to quinoline: a review. *Eur. J. Med. Chem.* **2019**, *164*, 121−170.

(6) Ramann, G.; Cowen, B. Recent advances in metal-free quinoline synthesis. *Molecules* **2016**, *21*, 986−1008.

(7) Russo, C. M.; Adhikari, A. A.; Wallach, D. R.; Fernandes, S.; Balch, A. N.; Kerr, W. G.; Chisholm, J. D. Synthesis and initial evaluation of quinoline-based inhibitors of the SH_2-containing inositol 5′-phosphatase (SHIP). *Bioorg. Med. Chem. Lett.* **2015**, *25*, 5344−5348.
(8) W. R., Carling; J. M., Elliott; E., Mezzogori; M. G. N., Russell; B. J., Williams *Quinoline Derivatives as Neurokinin Receptor Antagonists*; Merck Sharp & Dohme Limited: Hoddesdon, Hertfordshire, 2006. WO/2006/013393.
(9) (a) Bhatt, H. G.; Agrawal, Y. K. Microwave-irradiated synthesis and antimicrobial activity of 2-phenyl-7-substitutedalkyl/arylamino-quinoline-4-carboxylic acid derivatives. *Med. Chem. Res.* **2010**, *19*, 392−402. (b) Michael, J. P. Quinoline, quinazoline and acridone alkaloids. *Nat. Prod. Rep.* **2005**, *22*, 627−646. (c) Michael, J. P. Quinoline, quinazoline and acridone alkaloids. *Nat. Prod. Rep.* **2004**, *21*, 650−668.
(10) (a) Wang, L.-M.; Hu, L.; Chen, H.-J.; Sui, Y.-Y.; Shen, W. One-pot synthesis of quinoline-4-carboxylic acid derivatives in water: Ytterbium perfluorooctanoate catalyzed Doebner reaction. *J. Fluorine Chem.* **2009**, *130*, 406−409. (b) Yu, X. Y.; Hill, J. M.; Yu, G.; Yang, Y.; Kluge, A. F.; Keith, D.; Finn, J.; Gallant, P.; Silverman, J.; Lim, A. A series of quinoline analogues as potent inhibitors of C. albicans prolyl tRNA synthetase. *Bioorg. Med. Chem. Lett.* **2001**, *11*, 541−544. (c) Döbner, O.; Gieseke, M. Ueber α-phenylcinchoninsäure und ihre homologen. *Justus Liebigs Ann. Chem.* **1887**, *242*, 290−300. (d) Allen, C. F. H.; Spangler, F. W.; Webster, E. R. 2-Aminopyridine and the doebner reaction. *J. Org. Chem.* **1951**, *16*, 17−20.
(11) (a) Duvelleroy, D.; Perrio, C.; Parisel, O.; Lasne, M.-C. Rapid synthesis of quinoline-4-carboxylic acid derivatives from arylimines and 2-substituted acrylates or acrylamides under indium (III) chloride and microwave activations. Scope and limitations of the reaction. *Org. Biomol. Chem.* **2005**, *3*, 3794−3804. (b) Gopalsamy, A.; Pallai, P. V. Combinatorial synthesis of heterocycles: Solid phase synthesis of 2-arylquinoline-4-carboxylic acid derivatives. *Tetrahedron Lett.* **1997**, *38*, 907−910.
(12) (a) Muscia, G. C.; Carnevale, J. P.; Bollini, M.; Asís, S. E. Microwave-assisted döbner synthesis of 2-phenylquinoline-4-carboxylic acids and their antiparasitic activities. *J. Heterocycl. Chem.* **2008**, *45*, 611−614. (b) Khan, I.; Shah, S. J. A.; Ejaz, S. A.; Ibrar, A.; Hameed, S.; Lecka, J.; Millán, J. L.; Sévigny, J.; Iqbal, J. Investigation of quinoline-4-carboxylic acid as a highly potent scaffold for the development of alkaline phosphatase inhibitors: synthesis, SAR analysis and molecular modelling studies. *RSC Adv.* **2015**, *5*, 64404−64413.
(13) Lackey, K.; Sternbach, D. D. Synthesis of substituted quinoline-4-carboxylic acids. *Synthesis* **1993**, *1993*, 993−997.
(14) Lv, Q.; Fang, L.; Wang, P.; Lu, C.; Lu, F. A simple one-pot synthesis of quinoline-4-carboxylic acid derivatives by Pfitzinger reaction of isatin with ketones in water. *Monatsh. Chem.* **2013**, *144*, 391−394.
(15) Saeed, A. E. M.; Elhadi, S. A. Synthesis of Some 2-Aryl- and 2,3-Diaryl-quinolin-4-carboxylic Acid Derivatives. *Synth. Commun.* **2011**, *41*, 1435−1443.
(16) Zhu, H.; Yang, R. F.; Yun, L. H.; Li, J. Facile and efficient synthesis of quinoline-4-carboxylic acids under microwave irradiation. *Chin. Chem. Lett.* **2010**, *21*, 35−38.
(17) Gao, Q.; Liu, S.; Wu, X.; Zhang, J.; Wu, A. Coproduct Promoted Povarov Reaction: Synthesis of Substituted Quinolines from Methyl Ketones, Arylamines, and α-Ketoesters. *J. Org. Chem.* **2015**, *80*, 5984−5991.
(18) Ghodsi, R.; Azizi, E.; Grazia Ferlin, M.; Pezzi, V.; Zarghi, A. Design, synthesis and biological evaluation of 4-(imidazolylmethyl)-2-aryl-quinoline derivatives as aromatase inhibitors and anti-breast cancer agents. *Lett. Drug Des. Discovery* **2016**, *13*, 89−97.
(19) Buchman, E. R.; Howton, D. R. Potential antimalarials. (2-phenyl-7,8-benzoquinalin-4)-α-piperidylcarbinos1. *J. Org. Chem.* **1949**, *14*, 895−899.
(20) Wang, D.; Astruc, D. Fast-growing field of magnetically recyclable nanocatalysts. *Chem. Rev.* **2014**, *114*, 6949−6985.
(21) Payra, S.; Saha, A.; Banerjee, S. Recent Advances on Fe-Based Magnetic Nanoparticles in Organic Transformations. *J. Nanosci. Nanotechnol.* **2017**, *17*, 4432−4448.
(22) Karimi, B.; Mansouri, F.; Mirzaei, H. M. Recent Applications of Magnetically Recoverable Nanocatalysts in C-C and C-X Coupling Reactions. *ChemCatChem* **2015**, *7*, 1736−1789.
(23) Shylesh, S.; Schünemann, V.; Thiel, W. R. Magnetically separable nanocatalysts: bridges between homogeneous and heterogeneous catalysis. *Angew. Chem., Int. Ed.* **2010**, *49*, 3428−3459.
(24) Mokhtary, M. Recent advances in catalysts immobilized on magnetic nanoparticles. *J. Iran. Chem. Soc.* **2016**, *13*, 1827−1845.
(25) Cheng, T.; Zhang, D.; Li, H.; Liu, G. Magnetically recoverable nanoparticles as efficient catalysts for organic transformations in aqueous medium. *Green Chem.* **2014**, *16*, 3401−3427.
(26) Lim, C. W.; Lee, I. S. Magnetically recyclable nanocatalyst systems for the organic reactions. *Nano Today* **2010**, *5*, 412−434.
(27) Iqbal, A.; Iqbal, K.; Li, B.; Gong, D.; Qin, W. Recent advances in iron nanoparticles: preparation, properties, biological and environmental application. *J. Nanosci. Nanotechnol.* **2017**, *17*, 4386−4409.
(28) Mrowczynski, R.; Nan, A.; Liebscher, J. Magnetic nanoparticle-supported organocatalysts−an efficient way of recycling and reuse. *RSC Adv.* **2014**, *4*, 5927−5952.
(29) Heravi, M. M.; Zadsirjan, V.; Dehghani, M.; Ahmadi, T. Towards click chemistry: Multicomponent reactions via combinations of name reactions. *Tetrahedron* **2018**, *74*, 3391−3457.
(30) Ibarra, I. A.; Islas-Jácome, A.; González-Zamora, E. Synthesis of polyheterocycles via multicomponent reactions. *Org. Biomol. Chem.* **2018**, *16*, 1402−1418.
(31) Ahmadi, T.; Mohammadi Ziarani, G.; Gholamzadeh, P.; Mollabagher, H. Recent advances in asymmetric multicomponent reactions (AMCRs). *Tetrahedron: Asymmetry* **2017**, *28*, 708−724.
(32) Zhang, D.; Hu, W. Asymmetric Multicomponent Reactions Based on Trapping of Active Intermediates. *Chem. Rec.* **2017**, *17*, 739−753.
(33) Filho, J. F. A.; Lemos, B. C.; de Souza, A. S.; Pinheiro, S.; Greco, S. J. Multicomponent Mannich reactions: General aspects, methodologies and applications. *Tetrahedron* **2017**, *73*, 6977−7004.
(34) Garbarino, S.; Ravelli, D.; Protti, S.; Basso, A. Photoinduced multicomponent reactions. *Angew. Chem., Int. Ed.* **2016**, *55*, 15476−15484.
(35) Levi, L.; Müller, T. J. J. Multicomponent syntheses of functional chromophores. *Chem. Soc. Rev.* **2016**, *45*, 2825−2846.
(36) Haji, M. Multicomponent reactions: A simple and efficient route to heterocyclic phosphonates. *Beilstein J. Org. Chem.* **2016**, *12*, 1269−1301.
(37) Zarganes-Tzitzikas, T.; Chandgude, A. L.; Dömling, A. Multicomponent reactions, union of MCRs and beyond. *Chem. Rec.* **2015**, *15*, 981−996.
(38) Oki, M.; Ikeda, H.; Toyota, S. Dimensiosolvatic effects. VI. Rates of ionization of 2-fluoro-4, 4, 5, 5-tetramethyl-1, 3-dioxolane: Dimensiosolvatic vs. hydrogen-bond effects. *Bull. Chem. Soc. Jpn.* **1999**, *72*, 1343−1349.
(39) (a) T. L., Gilchrist *Heterocyclic Chemistry*; Prentice Hall, 1997. (b) Erhardt, J. M.; Wuest, J. D. Transfer of hydrogen from orthoamides. Reduction of protons to molecular hydrogen. *J. Am. Chem. Soc.* **1980**, *102*, 6363−6364. (c) Atkins, T. J. Tricyclic trisaminomethanes. *J. Am. Chem. Soc.* **1980**, *102*, 6364−6365. (d) Erhardt, J. M.; Grover, E. R.; Wuest, J. D. Transfer of hydrogen from orthoamides. Synthesis, structure, and reactions of hexahydro-6bH-2a, 4a, 6a-triazacyclopenta [cd] pentalene and perhydro-3a, 6a, 9a-triazaphenalene. *J. Am. Chem. Soc.* **1980**, *102*, 6365−6369.
(40) Igor, V. *Alabugin, Stereoelectronic Effects: A Bridge between Structure and Reactivity*; John Wiley & Sons, Ltd, 2016.
(41) Curran, D. P.; Suh, Y.-G. Selective mono-Claisen rearrangement of carbohydrate glycals. A chemical consequence of the vinylogous anomeric effect. *Carbohydr. Res.* **1987**, *171*, 161−191.
(42) Denmark, S. E.; Dappen, M. S.; Sear, N. L.; Jacobs, R. T. The vinylogous anomeric effect in 3-alkyl-2-chlorocyclohexanone oximes and oxime ethers. *J. Am. Chem. Soc.* **1990**, *112*, 3466−3474.

https://dx.doi.org/10.1021/acsomega.9b03277
ACS Omega 2020, 5, 3207−3217

(43) Jäkel, C.; Dötz, K. H. Organotransition metal modified sugars. *J. Organomet. Chem.* **2001**, *624*, 172−185.
(44) Drew, M. D.; Wall, M. C.; Kim, J. T. Stereoselective propargylation of glycals with allenyltributyltin (IV) via a Ferrier type reaction. *Tetrahedron Lett.* **2012**, *53*, 2833−2836.
(45) Nowacki, A.; Walczak, D.; Liberek, B. Fully acetylated 1, 5-anhydro-2-deoxypent-1-enitols and 1, 5-anhydro-2, 6-dideoxyhex-1-enitols in DFT level theory conformational studies. *Carbohydr. Res.* **2012**, *352*, 177−185.
(46) Nowacki, A.; Liberek, B. Acetylated methyl 1, 2-dideoxyhex-1-enopyranuronates in density functional theory conformational studies. *Carbohydr. Res.* **2013**, *371*, 1−7.
(47) Asgari, M.; Nori-Shargh, D. Exploring the impacts of the vinylogous anomeric effect on the synchronous early and late transition states of the hydrogen molecule elimination reactions of cis-3,6-dihalocyclohexa-1,4-dienes. *Struct. Chem.* **2017**, *28*, 1803−1814.
(48) Nowacki, A.; Liberek, B. Comparative conformational studies of 3, 4, 6-tri-O-acetyl-1, 5-anhydro-2-deoxyhex-1-enitols at the DFT level. *Carbohydr. Res.* **2018**, *462*, 13−27.
(49) Ferrier, R. J.; Sankey, G. H. Unsaturated carbohydrates. Part VII. The preference shown by allylic ester groupings on pyranoid rings for the quasi-axial orientation. *J. Chem. Soc.* **1966**, *0*, 2345−2349.
(50) Katritzky, A. R.; Steel, P. J.; Denisenko, S. N. X-Ray crystallographic evidence for a vinylogous anomeric effect in benzotriazole-substituted heterocycles. *Tetrahedron* **2001**, *57*, 3309−3314.
(51) Atashkar, B.; Zolfigol, M. A.; Mallakpour, S. Applications of biological urea-based catalysts in chemical processes. *Mol. Catal.* **2018**, *452*, 192−246.
(52) Zolfigol, M. A.; Navazeni, M.; Yarie, M.; Ayazi-Nasrabadi, R. Application of a biological-based nanomagnetic catalyst in the synthesis of bis-pyrazols and pyrano [3, 2-c] pyrazoles. *Appl. Organomet. Chem.* **2017**, *31*, No. e3633.
(53) Mohammadi, L.; Zolfigol, M. A.; Khazaei, A.; Yarie, M.; Ansari, S.; Azizian, S.; Khosravi, M. Synthesis of nanomagnetic supported thiourea−copper (I) catalyst and its application in the synthesis of triazoles and benzamides. *Appl. Organomet. Chem.* **2017**, *32*, No. e3933.
(54) Zolfigol, M. A.; Navazeni, M.; Yarie, M.; Ayazi-Nasrabadi, R. Application of biological-based nano and nano magnetic catalysts in the preparation of arylbispyranylmethanes. *RSC Adv.* **2016**, *6*, 92862−92868.
(55) Karimi, F.; Zolfigol, M. A.; Yarie, M. A novel and reusable ionically tagged nanomagnetic catalyst: Application for the preparation of 2-amino-6-(2-oxo-2H-chromen-3-yl)-4-arylnicotinonitriles via vinylogous anomeric based oxidation. *Mol. Catal.* **2019**, *463*, 20−29.
(56) Safaiee, M.; Ebrahimghasri, B.; Zolfigol, M. A.; Baghery, S.; Khoshnood, A.; Alonso, D. A. Synthesis and application of chitosan supported vanadium oxo in the synthesis of 1, 4-dihydropyridines and 2, 4, 6-triarylpyridines via anomeric based oxidation. *New J. Chem.* **2018**, *42*, 12539−12548.
(57) Zolfigol, M. A.; Khazaei, A.; Karimitabar, F.; Hamidi, M.; Maleki, F.; Aghabarari, B.; Sefat, F.; Mozafari, M. Synthesis of Indolo [3, 2-b] carbazoles via an Anomeric-Based Oxidation Process: A Combined Experimental and Computational Strategy. *J. Heterocycl. Chem.c* **2018**, *55*, 1061−1068.
(58) Noura, S.; Ghorbani, M.; Zolfigol, M. A.; Narimani, M.; Yarie, M.; Oftadeh, M. Biological based (nano) gelatoric ionic liquids (NGILs): Application as catalysts in the synthesis of a substituted pyrazole via vinylogous anomeric based oxidation. *J. Mol. Liq.* **2018**, *271*, 778−785.
(59) Zolfigol, M. A.; Safaiee, M.; Ebrahimghasri, B.; Baghery, S.; Alaie, S.; Kiafar, M.; Taherpour, A.; Bayat, Y.; Asgari, A. Application of novel nanostructured dinitropyrazine molten salt catalyst for the synthesis of sulfanylpyridines via anomeric based oxidation. *J. Iran. Chem. Soc.* **2017**, *14*, 1839−1852.
(60) Babaee, S.; Zolfigol, M. A.; Zarei, M.; Zamanian, J. 1, 10-Phenanthroline-Based Molten Salt as a Bifunctional Sulfonic Acid Catalyst: Application to the Synthesis of N-Heterocycle Compounds via Anomeric Based Oxidation. *ChemistrySelect* **2018**, *3*, 8947−8954.
(61) Baghery, S.; Zolfigol, M. A.; Maleki, F. [TEATNM] and [TEATCM] as novel catalysts for the synthesis of pyridine-3, 5-dicarbonitriles via anomeric-based oxidation. *New J. Chem.* **2017**, *41*, 9276−9290.
(62) (a) Yarie, M. Catalytic anomeric based oxidation. *Iran. J. Catal.* **2017**, *7*, 85−88. (b) Yarie, M. Catalytic vinylogous anomeric based oxidation (Part I). *Iran. J. Catal.* **2020**, article in press.
(63) Gholinejad, M.; Afrasi, M.; Nikfarjam, N.; Nájera, C. Magnetic crosslinked copoly(ionic liquid) nanohydrogel supported palladium nanoparticles as efficient catalysts for the selective aerobic oxidation of alcohols. *Appl. Catal., A* **2018**, *563*, 185−195.
(64) Qu, S.; Yang, H.; Ren, D.; Kan, S.; Zou, G.; Li, D.; Li, M. Magnetite nanoparticles prepared by precipitation from partially reduced ferric chloride aqueous solutions. *J. Colloid Interface Sci.* **1999**, *215*, 190−192.

https://dx.doi.org/10.1021/acsomega.9b03277
ACS Omega 2020, 5, 3207−3217